

The Combined effects of Blast and Fragment impacts on Textiles

G. Kechagiadakis¹, D. Lecompte¹ and W. Paepegem²

¹Royal Military Academy, Avenue de la Renaissance 30, 1000, Brussels, Belgium
georgios.kechagiadakis@mil.be

²Department of Materials, Textiles and Chemical Engineering, Ghent University,
Technologiepark–Zwijnaarde 46, B-9502 Zwijnaarde, Belgium

Abstract. Explosion protection of Personal Protective Equipment is a widely discussed topic in the Defence sector albeit largely misrepresented experimentally. Oversimplified STANAG 2920 single-impact tests and unregulated field blast tests with limited repeatability and ambiguous results, hinder a comprehensive understanding of the problem: the synchronised impact of fragments and a blast wave on a given target. A laboratory experimental setup capable of simulating the combined effects of blast and fragment impacts of a wide range of explosive devices at a defined stand-off distance from a target is developed. A single 1.1g FSP is ejected using a 5.56mm weapon system; tautochronously, a blast wave is generated in an explosives driven shock tube. The two loads are synchronised based on a predetermined simulated stand-off distance. Aramid dry fabrics are tested in different combinations of fragment impacting velocity, blast overpressure and time interval between the two loads, to evaluate their fragment impact resistance in the presence of blast. The tests reveal a time-dependent material ballistic resistance, influenced positively or negatively by the material's oscillating phase. The blast overpressure/impulse acts as an amplifying factor, exacerbating the synergistic effects observed at different time intervals.

1. INTRODUCTION

Protection against the effects of explosions is a topic that has received extensive attention from the scientific community over the past decades. Many military or civilian applications involve the potential exposure to explosive loads of people, vehicles, or infrastructure. Certain test procedures were developed in order to ensure a basic level of protection can be achieved. Standardised ballistic impact tests incorporating fragment simulants have been at the forefront of fragment protection for personal protective equipment. These standards provide practical and clear instructions and can produce repetitive and comparable results. However, these methods often present an oversimplified view of reality. Explosions are complex multi-physics threats that can affect the surrounding space in many ways. The blast is a rapidly expanding shockwave that exerts immense crushing pressure, transmitting high impulse loads. The shattering of the casing can produce fragments, debris, pebbles and dirt from the surrounding area can be propelled at lethal speeds causing damage. Explosions are exothermic reactions that generate high heat that can ignite flammable materials and cause burns. These phenomena manifest in a successive order that can span from microseconds to minutes and have synergistic effects. This means that by limiting the analysis to one of these aspects the conclusions may have little connection to the initial physical problem.

In literature, there have been a few articles describing such synergistic effects between loads that result from explosions. Combined blast and fragment loading can cause more severe damage than the sum of individual blast and fragment damage [1, 2, 3]. Many researchers consistently highlight the necessity of moving beyond single-threat assessments to integrated approaches that account for the combined effects. [4, 5, 6]. Numerical simulations are crucial tools for analysing combined blast and fragment loading scenarios [2, 7]. 3D Finite Element simulations present improved accuracy over 2D F.E. simulations, as they capture the complex interactions between blast waves, fragments and target structures [7]. Experimental studies were also used as essential tools for validating numerical models and for evaluating the material and structural responses to combined loads [8, 9, 10]. Many of the published articles propose tests in which the combined blast and fragment impact loads are generated using high explosives and pre-cut fragments [8, 9, 10, 11, 12, 13, 14, 15, 16, 17].

Regarding the post-treatment of the evaluated material and structural response, this includes studying the behaviour of S-2 glass/epoxy composite laminates [11], sandwich panels with different core configurations [9, 12], polyurea-coated steel plates [10, 13], reinforced concrete [2, 3], and UHMWPE composites [14, 18]. Failure mechanisms and damage patterns under combined loads are analysed to promote design and protection strategies [3, 9, 12, 15].

Aramid fabrics have been the most popular textiles for PPE in the past decades. High toughness-to-density ratio of aramid fibres give aramid dry fabrics increased impact absorption capacity. The

woven structure of aramid fabrics is crucial to enhancing their impact resistance. The interlaced yarns create an entangled network that disperses the energy from projectile impacts through a frictional yarn-to-yarn motion. Aramid fabrics are used extensively in personal protective equipment against explosions. Even though their multi-hit fragmentation resistance has been analysed extensively [19, 20], their impact performance in the presence of blast loads hasn't been documented. Their near instantaneous reaction times make them difficult to hold in place while high impulse testing. What is more, until recently the problem of applying the combination of a blast wave in conjunction with a single or multiple fragments, consistently, has been largely an unsolved problem. In this article, a consistent, highly controllable, synchronised blast wave and single fragment impact loading test is presented.

2. METHODS

An experimental setup that can simulate a range of explosive events in a consistent and controllable manner is developed in the Department of Structures and effects of Explosions of the Royal Military Academy of Belgium. The setup ensures the independent control of specific characteristics that define the conditions of an explosion:

- The explosive device:
 - The blast wave has a specific overpressure/impulse at a given stand-off distance
 - The fragment generation yields specific fragment masses/velocities
- The Stand-off Distance:
 - The blast and the fragments travel at different speeds, hence the time interval between these loads correspond to a specific stand-off distance.

These three constituents can characterise an explosive event.

The Blast: The blast wave is generated using an Explosive Driven Shock Tube (EDST). This ensures that the blast wave has consistently repeatable pressure profiles with only a small charge as an input. The applied blast load is also near-planar, free of reflections from near surfaces as it is guided onto the target through the tube. The clamping system is places 20mm away from the tube's end.

The Fragments: A fragment simulant can be propelled using a pyrotechnic launcher. The universal receiver supports barrels from 5.56mm to 12.7mm. This enables the use of a wide range of fragment simulants including NATO's Fragment Simulating Projectiles (except the 20mm version) and other commercial or custom-made projectiles. What is more, with the use of a velocity base light gate system, the projectile velocity can be precisely measured and the impact point can be accurately defined.

The third parameter is the time interval between the loads, which is calculated using the projectile and the blast wave velocities.

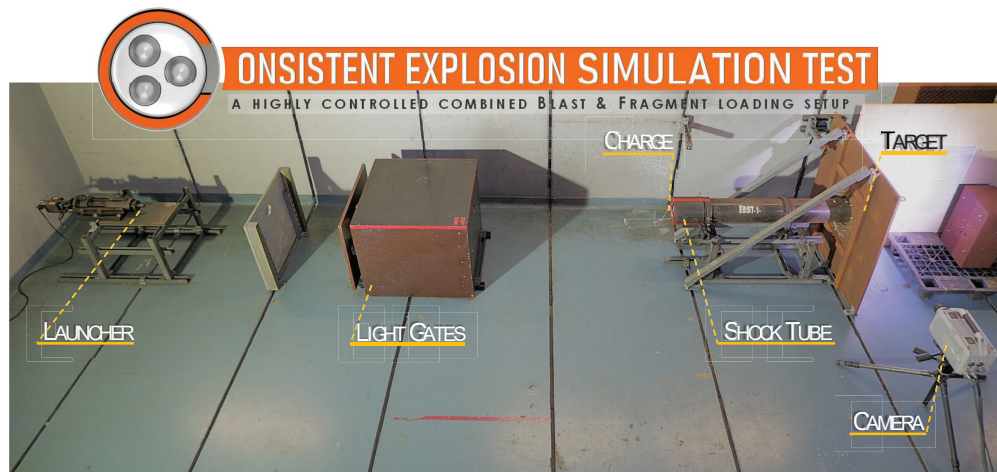


Figure 1. The Combined Blast and Fragment Loading setup is presented: A weapon system is used to launch the FSP through the Blast Tube on to the target. An explosive charge is activated at the front end of the Blast Tube generating a planar blast wave at the target. The two systems are timed for a synchronised arrival of combined loads with specific, impacting velocity, blast overpressure and time interval between the loads.

2.1 Materials

An extensive experimental campaign of 55 combined blast loading and fragment impact tests is conducted on samples comprising 15 layers of plain weave K29 Kevlar fabrics with a total areal density of 2.9kg/m^2 . This specific dry fabric type was used in previous studies and it was selected for comparison purposes. The fabric is supported using a $\text{Ø}135\text{mm}$ circular clamping frame which it comprises a neck flange, a support frame and an outer ring. The fabric is pushed through the outer ring by the neck flange as the outer ring is tightened using 10x M10 screws, and the fabric is slightly stretched and auto-aligned with the blast tube.

2.2 Loads

The proposed setup is capable of a broad range of output loads. The test case proposed by the International Mine Action Standards (IMAS) 10.30 was selected as it provides detailed requirements including the explosive device, the equivalent fragmentation resistance when considering the 1.102g FSP and the stand-off distance from the target [21]. In the IMAS 10.30, a test case of an accidental detonation of a PMN anti-personnel landmine is described, placed 60cm away from the torso of a deminer. The standard also determines also the minimum threshold of the ballistic resistance of the deminer's vest of 450m/s, tested according to NATO's STANAG 2920. The PMN is the largest antipersonnel blast landmine, containing 240g of TNT. Based on the 240g TNT charge and the 60cm stand-off distance, a blast wave with an incident/reflected overpressure in the proximity of 1.4/8.9MPa was calculated using the Kingery-Bulmash equations [22].

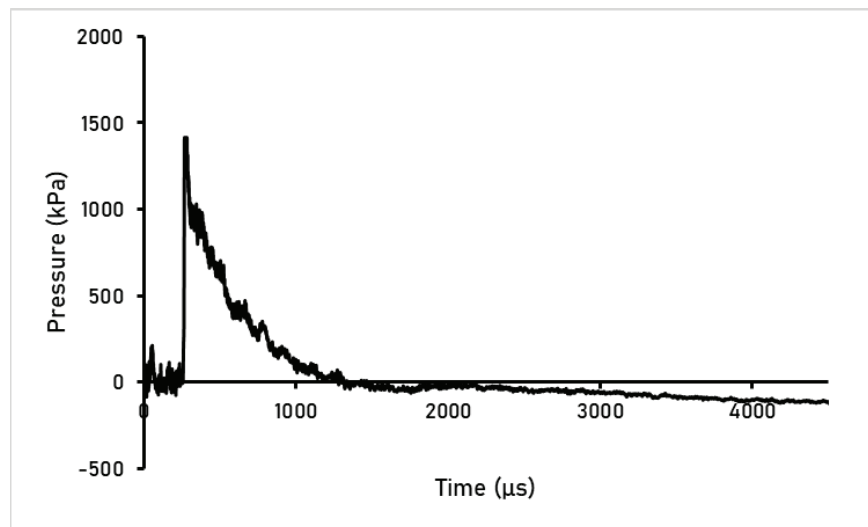


Figure 2. The incident pressure of the blast wave travelling through the Blast Tube is measured 10cm before the end of the tube. No target was in place for this measurement.

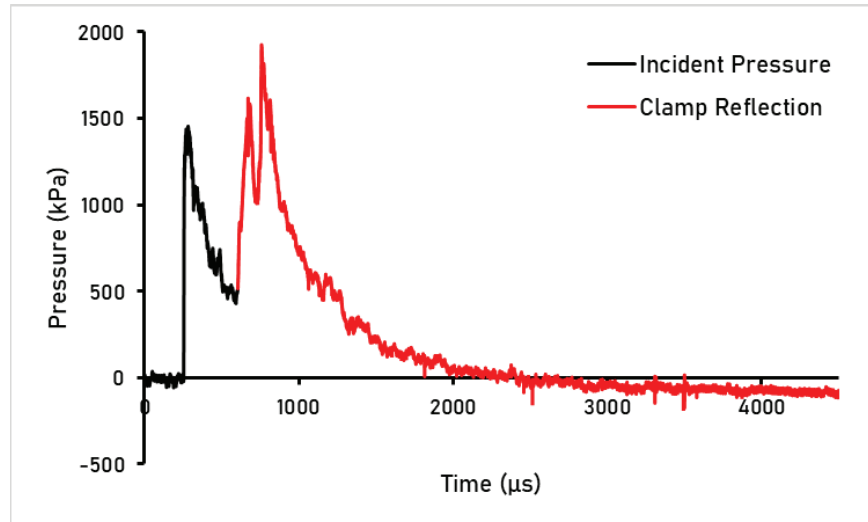


Figure 3. The incident pressure of the blast wave travelling through the Blast Tube is measured 10cm before the end of the tube. In this case, the target is causing reflections, which are distinguishable in the pressure measurements with red line.

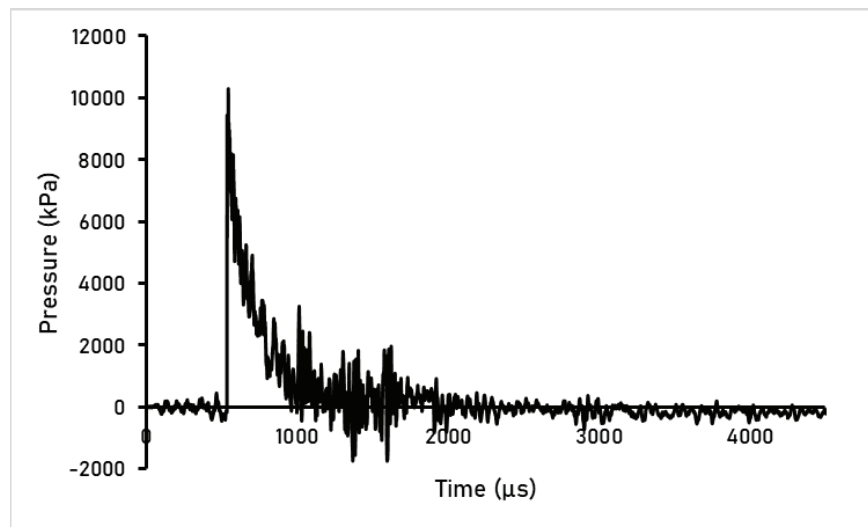


Figure 4. The reflected pressure measured at the exit of the Blast Tube.

3. RESULTS

The response of the aramid fabric under blast loads goes through phases. Initially, the fabric reacts almost instantaneously with the arrival of the blast wave. Longitudinal and transverse waves are generated from the edges of the free surface adjacent to the clamp travelling towards the centre. A truncated cone gradually forms, with the central part of the fabric remaining flat. As the stress waves continue to propagate, the fabric assumes a fully conical shape and its out-of-plane velocity maximises at about 250m/s. At this moment, the clamping forces are insufficient to retain the accelerated fabric, resulting in significant slippage with a magnitude of 16-17mm in the warp/weft directions and about 6-8mm at 45°, 135°, 225° and 335° [23]. The tip of the cone backlashes as the rest of the fabric continues to move forward, slipping through the clamping system. This results in the formation of a hemi-ellipsoid which remains until the end of the blast's positive phase. Beyond that point the fabric gets sucked backwards during the negative phase.

Aramid fabric present a phase dependent modulation in their ballistic resistance.

The time interval between the two loads appears to be a critical factor when it comes to the outcome of a combined loading event. In this study, the time interval is considered using the arrival of the blast wave as a reference. With this in mind, when the blast wave arrives first this results in positive time intervals. When the fragment simulant arrives first, the time interval assumes negative values. Of the 55 total combined blast loading and fragment impact tests, 9 have a negative time interval. As ballistic impact is a phenomenon that takes place within tens of microseconds, the fragment impact concludes before the blast wave may have any effect on the fabric. Furthermore, the blast wave at the levels examined (4.6MPa-10MPa) the fabric is able to withstand the loads with only a mild tearing of the first of the 15 layers at the boundaries. Even after a full perforation, the fabric remained unaffected by the subsequent blast load.

In the case of positive time intervals, two very distinct material behaviours are observed. Combined loading tests with short time intervals, below 150 μ s, result in elevated ballistic performance. The ballistic limit shows an increase of 18% from a base value of 483m/s without the blast, to 570m/s. On the other hand, time intervals over 150 μ s up to 516 μ s, exhibit a critical decrease in the ballistic performance of the aramid fabric by 17%, from 483m/s to 413m/s. The results can be seen in the table 1. This is a major security concern as in many cases textiles are being used as a means of protection against fragmentation resulting from explosions. Given that this critical time interval corresponds to a range of stand-off distances, this means that at certain distances the ballistic resistance may demonstrate critically low performance.

The fabric's variable ballistic performance is accounted for three material changes:

- The damage accumulation that resulting from the applied loads exceeding locally the strength limit of the aramid.
- The superposition of stress energy deposit due to the application of a near-uniform pressure over the fabric's surface during fragment impact.
- The dynamic material response from two consecutive loads that can result in an increased or decreased relative impacting velocity between the fragment and the fabric, accelerated previously by the blast. Previous studies indicated that this mechanism is very impactful when it comes to flexible materials under multiple impulsive loads. Additionally, multiple impacts aligned to the material's natural frequencies become resonant impacts and have increased potential in resulting in catastrophic failure [20].

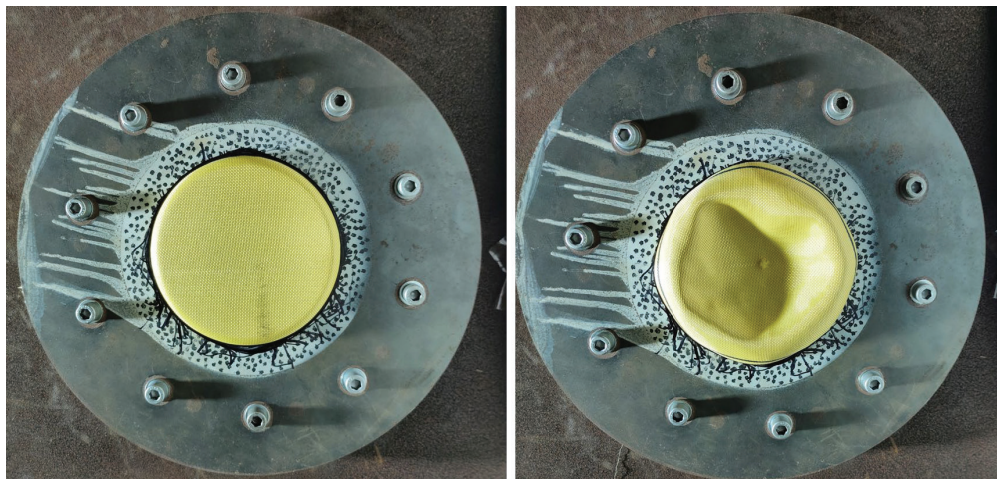


Figure 5. An aramid fabric sample before and after being tested with the combined blast and fragment impact loading test.

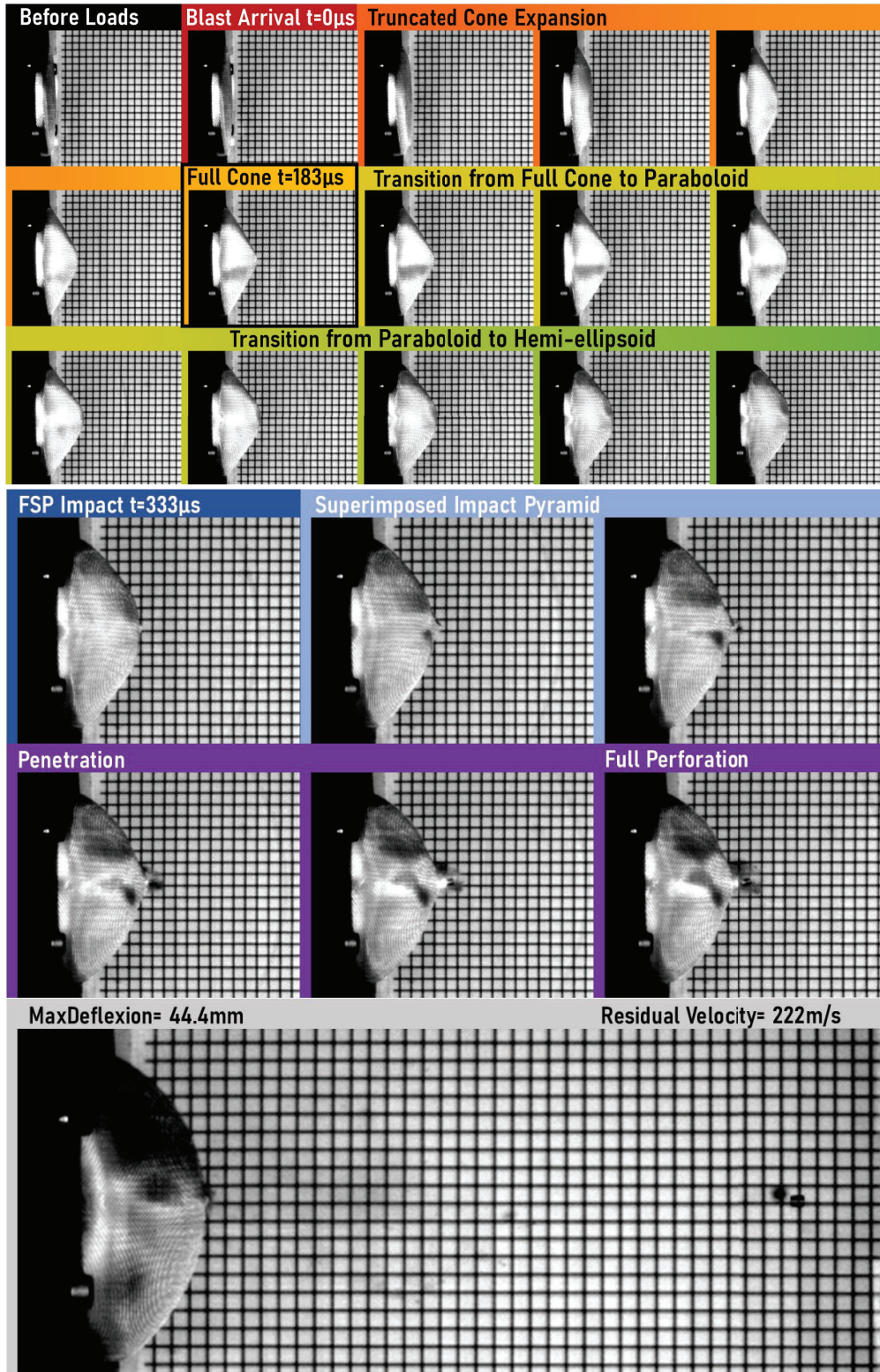


Figure 6. Consecutive frames of a combined blast and fragment impact on an aramid fabric. The fabric undergoes various phases. At $t=333\mu s$ after the arrival of the blast wave, the FSP arrives on the target.

Table 1. Test results from combined blast and fragment impact tests at different time intervals;
 Negative: [-210 μ s,-17 μ s], Positive:[0,150 μ s] and Positive:[150 μ s, 516 μ s].

(-210) - (-17) μ s		0-150 μ s		150-516 μ s	
Impacting velocity (m/s)	Result	Impacting velocity (m/s)	Result	Impacting velocity (m/s)	Result
571	P	580	NP	399	NP
562	P	-	P	447	P
600	P	574	P	449	NP
577	P	637	P	438	P
565	P	441	NP	449	P
580	P	472	NP	454	P
569	P	526	NP	449	P
534	P	524	NP	502	P
434	NP	561	NP	413	NP
		572	P	473	P
		566	NP	470	P
		574	NP	396	NP
		586	P	434	P
		580	P	413	NP
		493	NP	417	P
		451	NP	437	P
		430	NP	449	P
		445	NP		
		492	NP		
		507	NP		
		563	P		
		437	NP		

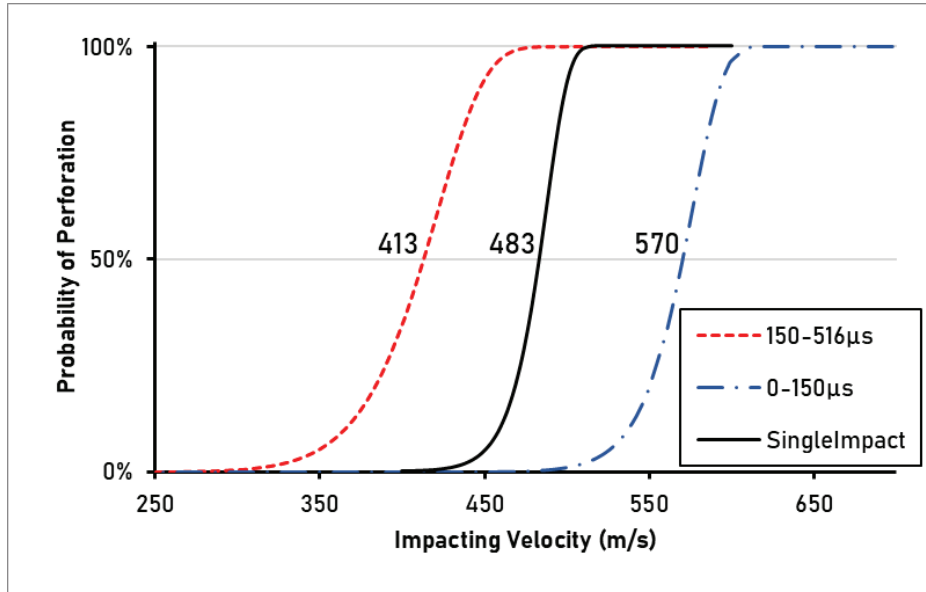


Figure 6. The probability of perforation density functions (Weibull) are fitted on the results from the Combined Blast and Fragment impact tests. The results are split into two distinct groups based on the time interval between the blast and the fragment impact. The results are compared with the base case in which only a single FSP is considered (without blast).

4. CONCLUSIONS

An experimental setup which allows the simulation of an explosive event in a laboratory scale is presented. The proposed setup is capable of generating a synchronised arrival of a planar blast wave and a fragment simulat impact. The three main parameters of the test - the impacting fragment velocity, the blast wave overpressure and the time of relative arrival of the two loads - can be controlled independently with millimetre and microsecond-level of accuracy.

The setup is used to test the fragment impact resistance of aramid fabrics in the presence of blast within a range of impacting velocities and time intervals, following the threat levels described by IMAS 10.30. The aramid fabrics reveal a phase-dependent ballistic resistance under the combined loads. The time interval between the loads plays a crucial role in the final outcome of a combined loading test. At short time intervals the ballistic resistance appears to increase greatly. At time intervals over 150 μ s, a significant drop in the ballistic resistance is observed.

Three major mechanisms of synergistic interactions between the blast and the fragment are identified: firstly, the damage accumulation from the blast wave influencing the subsequent fragment impact; secondly, the elevated stress-strain energy density due to the continuous application of the blast wave during the fragment impact; and finally, the change of the kinetic state of the fabric after the arrival of the blast wave can reduce or increase the relative impacting velocity of the projectile with respect to the moving fabric resulting in stronger or weaker impact.

References

- [1] Li, J., Huang, C., Ma, T., Huang, X., Li, W., Liu, M. Numerical investigation of composite laminate subjected to combined loadings with blast and fragments. *Composite Structures* 214 (2019), 335–347.
- [2] Nyström, U., Gylltoft, K. Numerical studies of the combined effects of blast and fragment loading. *International Journal of Impact Engineering* 36 (2009), 995–1005.
- [3] Goswami, A., Ganesh, T., Adhikary, S.D., 2022. RC structures subjected to combined blast and fragment impact loading: A state-of-the-art review on the present and the future outlook. *International Journal of Impact Engineering* 170 (2022), 104355.
- [4] Grisaro, H.Y., Dancygier, A.N., 2018. Characteristics of combined blast and fragments loading. *International Journal of Impact Engineering* 116 (2018), 51–64.
- [5] Grisaro, H.Y., Benamou, D., Dancygier, A.N. Investigation of blast and fragmentation loading characteristics – Field tests. *Engineering Structures* 167 (2018), 363–375.
- [6] Mellen, P., Shanahan, C., Bennett, T. Blast and fragmentation loading indicative of a VBIED surrogate for structural panel response analysis. *International Journal of Impact Engineering* 126 (2019), 172–184.
- [7] Grisaro, H., Dancygier, A.N. Numerical study of velocity distribution of fragments caused by explosion of a cylindrical cased charge. *International Journal of Impact Engineering* 86 (2015), 1–12.
- [8] Li, D., Hou, H., Chen, C., Zhu, X., Li, M., Yi, Q. Experimental study on the combined damage of multi-layered composite structures subjected to close-range explosion of simulated warheads. *International Journal of Impact Engineering* 114 (2018), 133–146.
- [9] Cai, S., Liu, J., Zhang, P., Li, C., Cheng, Y., Chen, C. Experimental study on failure mechanisms of sandwich panels with multi-layered aluminum foam/UHMWPE laminate core under combined blast and fragments loading. *Thin-Walled Structures* 159 (2021), 107227.
- [10] Wu, G., Wang, X., Ji, C., Liu, Q., Xie, X., Zhao, C., Liu, P. Damage response of polyurea-coated steel plates under combined blast and fragments loading. *Journal of Constructional Steel Research* 190 (2022), 107126.
- [11] Li, J., Huang, C., Ma, T., Huang, X., Li, W., Liu, M. Numerical investigation of composite laminate subjected to combined loadings with blast and fragments. *Composite Structures* 214 (2019), 335–347.
- [12] Zhang, P., Mo, D., Ge, X., Wang, H., Zhang, C., Cheng, Y., Liu, J. Experimental investigation into the synergetic damage of foam-filled and unfilled corrugated core hybrid sandwich panels under combined blast and fragment loading. *Composite Structures* 299 (2022), 116089.
- [13] Zhang, L., Ji, C., Wang, X., Wang, Y., Wu, G., Zhu, H., Han, Z. Strengthening and converse strengthening effects of polyurea layer on polyurea–steel composite structure subjected to combined actions of blast and fragments. *Thin-Walled Structures* 178 (2022), 109527.
- [14] Liang, M., Zhou, M., Li, X., Lin, Y., Lu, F. Synergistic effect of combined blast loads on UHMWPE fiber mesh reinforced polyurea composites. *International Journal of Impact Engineering* 183 (2024), 104804.

- [15] Cai, S., Liu, J., Zhang, P., Li, C., Cheng, Y., Chen, C. Experimental study on failure mechanisms of sandwich panels with multi-layered aluminum foam/UHMWPE laminate core under combined blast and fragments loading. *Thin-Walled Structures* 159 (2021), 107227.
- [16] Zhang, P., Wang, K., Hu, P., Li, Z., Chen, G., Cheng, Y. Experimental study on the synergetic damage of sandwich panel with armored hybrid core under combined blast and fragment loading. *Thin-Walled Structures* 199 (2024), 111814.
- [17] Wu, G., Wang, X., Ji, C., Liu, Q., Gao, Z., Zhang, K., Zhao, C. Experimental and numerical simulation study on polyurea-coated fuel tank subjected to combined action of blast shock waves and fragments. *Thin-Walled Structures* 169 (2021), 108436.
- [18] Zhao, C.-Z., Qiang, L.-S., Zhang, R., Zhang, Q.-C., Zhong, J.-Y., Zhao, Z.-Y., Lu, T.J. Dynamic response of UHMWPE plates under combined shock and fragment loading. *Defence Technology* 27 (2023), 9–23.
- [19] Kechagiadakis, G., Lecompte, D., Van Paepegem, W., Coghe, F., Pirlot, M. Experimental evaluation of the ballistic resistance of aramid fabrics under near simultaneous multiple fragment impacts. *International Journal of Impact Engineering* 180 (2023), 104675.
- [20] Kechagiadakis, G., Lecompte, D., Van Paepegem, W., Coghe, F., Pirlot, M. Near simultaneous multiple fragment impacts on aramid fabrics: Effects of velocity, dispersion and time intervals. *International Journal of Impact Engineering* 185 (2024), 104830.
- [21] International Mine Action Standards 10.30. 2nd Edition, Amendment 5 (2023)
- [22] Kingery, C., Bulmash, G. Airblast parameters from TNT spherical air burst and hemispherical surface burst. Technical report ARBL-TR-02555 (1984).
- [23] Kechagiadakis, G., Lecompte, D., Van Paepegem. Sliding Boundaries in Finite Element modelling of soft materials under blast loads.